laxation of entanglements or perhaps by still greater long-range motions. Great differences in the cross-linking degrees can influence also the shape of the glass–rubber transition; the steepness of the retardation (L) and relaxation (H) spectra in this range is lower for highly cross-linked samples.

Acknowledgments. This work was supported in part by a grant from the National Science Foundation. We are indebted to Mr. Chiu-Ping Wong for preparing the computer program for the double transducer and torsion pendulum data. Furthermore the help of Miss Christina A. Gibbs, Miss Linda L. Petersen, Mrs. Nancy R. Vebber, and Miss Linda J. DeAngelis with the calculations and of Mrs. Garnie E. Mullen with the writing of the manuscript is gratefully acknowledged.

Deformation and Structure of Cylindrical "Spherulites" in Transcrystalline Polyethylene. Detection and Characterization of the Pseudomonoclinic Crystalline Component

C. Gieniewski and R. S. Moore

Bell Telephone Laboratories, Inc., Murray Hill, New Jersey 07974.
Received April 3, 1969

ABSTRACT: The crystalline structure and the deformation of cylindrical spherulites were studied in transcrystalline polyethylene. The experimental results indicate that the cylindrical "spherulites" are comprised of symmetrically packed, specifically oriented lamellae which have their longest axis aligned predominantly with the long axis of the cylindrical spherulites, the long axis being normal to the plane of the polymer film. From the crystallographic data it is concluded that the banded structure observed is the result of lamellar cooperative twisting similar to that found in symmetric spherulites. The distribution of orientations observed in the X-ray diagrams supports evidence in the photomicrographs which suggests that the cylindrical "spherulites" start to grow as spheres in an umbrella-like fashion until they impinge on neighboring spherulites. From then on their growth is restricted to one direction. Under the force of lateral stretching (draw direction normal to the long axis of the spherulites) the lamellar ribbons within the spherulites are first found to spread apart to a certain degree with the retention of over-all cooperative twisting. Subsequently they tilt, aligning their longest axis with the direction of stretching, pull out from the spherulitic aggregates, and untwist. Soon thereafter, reorientation into a new fiberlike structure occurs in which the unit cell c axis is preferentially oriented in the draw direction, as evidenced by the X-ray diffraction results. A pseudo-monoclinic crystalline component was detected in this transcrystalline polyethylene and the unit cell parameters were established. This pseudomonoclinic component was also observed in all forms of crystalline polyethylene which we investigated and is considered likely to be a feature common to all polyethylenes. One possible manner of formation of this component is given in terms of a slightly different packing of the folded polymer chains in a somewhat strained lattice array. The proposed pseudomonoclinic unit cell accounts for all "extra" reflections observed in X-ray diagrams of polyethylenes we have investigated.

From the voluminous work done on crystalline morphology in polyethylene it is known that the polymer chains fold upon themselves to form lamellar crystallites[1] which have ribbonlike geometric structure. Crystallization in bulk is commonly found to occur in the form of spherulites composed of lamellar fibrils.[2–4] The unit cell b axis (for structure, see Bunn)[5] in polyethylene spherulites is predominantly oriented along the longest lamellar axis (which is also the growth axis) of the lamellar fibrils, and the fibrils lie predominantly along the spherulite radii.[1–4]

Among the several somewhat different habits of crystallization in high polymers is a so-called "transcrystalline," or "rowlike," morphology[6–9] which was observed some time ago. This morphology is characterized by the presence of cylindrical crystalline aggregates (cylindrical "spherulites")[9] each of which (on the average) has its long axis predominantly perpendicular to the flat, large surfaces of the polymer sheet. The cylindrical "spherulites" have been found to form by growth from the molding surfaces into the polymer melt from both sides,[6] by nucleation within the molten polymer mass,[9] or by growth in one direction only, as shown in Figures 1, 2a, and 2b. (The figures are discussed in more detail later.)

X-Ray diffraction and birefringence studies[9,10] have revealed that the orthorhombic unit cell b axis and the longest lamellar axis are preferentially oriented parallel

(1) A. Keller, *J. Polym. Sci.*, **17**, 351 (1955).
(2) A. Keller, *Phil. Mag.*, [8] **2**, 1171 (1957).
(3) A. Keller and A. O'Connor, *Discussions Faraday Soc.*, **25**, 114 (1958).
(4) H. D. Keith, "The Physics and Chemistry of the Organic Solid State," D. Fox, Ed., Interscience Publishers, New York, N. Y., 1963, Chapter 8.
(5) C. W. Bunn, *Trans. Faraday Soc.*, **35**, 482 (1939).
(6) E. Jenckel, E. Teege, and W. Hindrichs, *Kolloid-Z.*, **129**, 19 (1952).
(7) R. J. Barriault and L. F. Gronholz, *J. Polym. Sci.*, **18**, 393 (1955).
(8) H. D. Keith and F. J. Padden, Jr., *ibid.*, **31**, 415 (1958).
(9) A. Keller, *ibid.*, **15**, 31 (1955).
(10) R. K. Eby, *J. Appl. Phys.*, **35**, 2720 (1964).

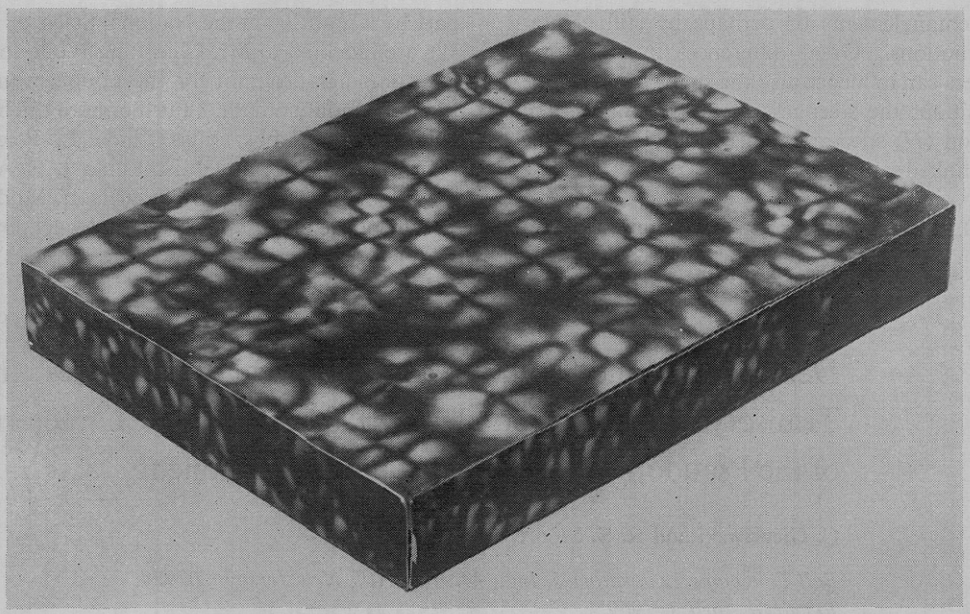

Figure 1. Pictorial representation of the sample of transcrystalline polyethylene used in our studies, with photomicrographic representation of the large surface (face) and of the edges as observed between crossed polarizers. Relative sample dimensions not to scale; relative face-to-edge magnification 4:1.

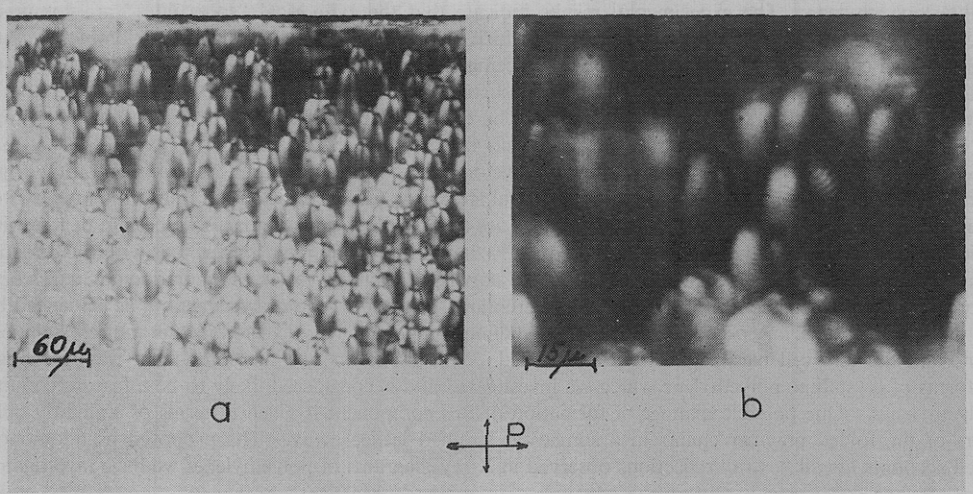

Figure 2. Crossed-polarizer photomicrographs of cylindrical spherulites looking normal to their long axis. The banded structure is visible in the photomicrograph of higher magnification. The plane of polarization of the incident light was horizontal and normal to the plane of the page.

to the long axis of the cylindrical "spherulites." Each of the spherulites is commonly found to exhibit a banded structure when viewed under a polarizing microscope.

In symmetric spherulites the banded structure is the result of lamellar cooperative twisting.[4,11–13] Because (as shown later) we find the same crystallographic orientation (unit cell *b* axis parallel to the long axis of a lamellar fibril) in the cylindrical "spherulites" as is found in symmetric spherulites, we conclude that the banded structure observed in the cylindrical "spherulites" also occurs from lamellar cooperative twisting, but in this case the twisting is restricted to being mainly parallel to the "spherulite" long axis.

A detailed understanding of the morphology of so-called transcrystalline polymers is of interest because materials of this type have been found to exhibit unusual properties with regard to diffusion,[10] adhesion,[14] and viscoelasticity.[15,16] It is likely that they also may exhibit unusual and highly anisotropic dielectric properties. The preparation of transcrystalline samples of polymers has recently become better understood to the extent that fairly thick sheets of high-density polyethylene can be prepared having transcrystalline morphology.[17]

Experimental Section

A 0.020-in.-thick sheet of transcrystalline Marlex 5003 polyethylene was prepared according to the method described elsewhere.[15] Thin specimens (some as thin as 10 μ)

(11) A. Keller, *J. Polym. Sci.*, **17**, 291 (1955).
(12) H. D. Keith and F. J. Padden, Jr., *ibid.*, **39**, 123 (1959).
(13) F. P. Price, *ibid.*, **37**, 71 (1959); **39**, 139 (1959).
(14) H. Schonhorn and F. W. Ryan, *J. Polym. Sci., Part A-2*, **6**, 231 (1968).
(15) T. K. Kwei, H. Schonhorn, and H. L. Frisch, *J. Appl. Phys.*, **38**, 2512 (1967).
(16) S. Matsuoka, J. H. Daane, H. E. Bair, and T. K. Kwei, *Polym. Lett.*, **6**, 87 (1968).
(17) H. M. Zupko, private communication (1968).

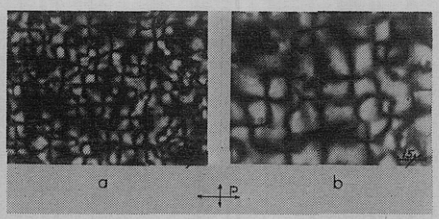

Figure 3. Crossed-polarizer photomicrographs of the cylindrical spherulites looking down the spherulite long axis. The plane of polarization of the incident light was horizontal and normal to the page.

were sectioned from the edge and the face of a 2 × 2 × 0.02 in. sample. Photomicrographs were obtained on a Unitron polarizing microscope. Cu Kα radiation from a General Electric X-ray apparatus was utilized to obtain X-ray diagrams, and an He–He CW gas laser with 6328-Å wavelength was used to obtain light scattering patterns. The X-ray beam size was relatively large (about 0.5 mm in diameter), though somewhat smaller than that of the laser beam (about 0.7 mm in diameter).

Compression molded films or sheets of Marlex 5003, 5035, 6050, and of DYNH-1 polyethylenes, as well as a mat of polyethylene single crystals, were used in X-ray studies of the pseudomonoclinic crystalline component.

Results and Discussion

A. Microscopy. Figure 1 shows the shape of our compression molded sample with photomicrographic representation of the flat face and of the edges as were observed between crossed polarizers. A more detailed description of the face and of the edges of this transcrystalline sample of polyethylene is given later.

Figure 2 shows representative photomicrographs of cross sections of the specimen photographed with the sample between crossed polaroids. The banded cylindrical "spherulites" are closely packed with their long axis vertical. The band or ring spacing (which equals one-half the twist distance for one complete fibril rotation) is about 1.5 μ, and the diameters of the cylindrical "spherulites" range between 10 and 20 μ, the majority of them being about 15 μ, so that the approximate ratio of the spherulite ring spacing to its diameter is 1:10. The length of the long spherulite axis cannot be determined precisely from these photomicrographs because of the tilted angle at which they were photographed, but it can be seen that they are at least 40 μ long.

Figure 3 shows crossed-polarizer photomicrographs from sections of the specimen cut parallel to the surface of the sheet; thus the cylindrical "spherulites" are viewed approximately end on. Here we observe a strong birefringence caused by the polarizability effects of (predominantly) the *a vs. c* axis. Instead of a maltese cross characteristic of regular polyethylene spherulites, we observe a quadrant type of cross. The photomicrographs add significant evidence about the orientational aspects of lamellar fibrils in the cylindrical "spherulites." They indicate that bundles of lamellae are closely packed and are oriented with their long axis parallel to the long axis of the "spherulites."

Figure 2 and also Figure 9 suggest that the twisting goes to the center of the "cap" at the top of the spherulites. Although twisting is not observed in Figure 3 it would be difficult to observe under these conditions

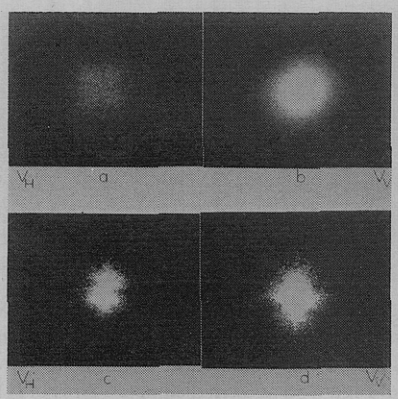

Figure 4. Laser light scattering patterns: Figure 4a is the V_H pattern with plane polarized light traveling down the spherulite long axis; Figure 4b is the V_V pattern per orientation of Figure 4a; Figure 4c is a V_H pattern with plane-polarized light along the spherulite long axis and horizontal in the picture; Figure 4d is the V_V pattern with orientation as in 4c. In all cases the laser beam was normal to the plane of the paper.

since only a small percentage of the fibrils (those in the "cap") of any cylindrical "spherulite" would lie parallel to the cross-sectional area. Further detailed investigation would be required to establish the details of any twisting in the "cap" section.

B. Laser Light Scattering. Laser light scattering patterns of thin specimens sectioned normal to the long axis of the cylindrical "spherulites" are shown in Figures 4a and 4b. Figure 4a (incident light horizontally polarized) is similar to the usual clover-leaf pattern[18,19] produced by polyethylene spherulites. Figure 4b shows a V_V light scattering pattern (polarization axes vertical) of the same specimen. This pattern indicates scattering similar to that found in symmetric spherulites. The specimen was sectioned normal to the long axis of the cylindrical "spherulites" so that the laser beam traveled predominantly down the long axis of the cylinders, and so was sensitive only to the cross sections of the cylindrical scatters.

With the laser beam directed perpendicular to the long axis of the cylindrical "spherulites" in the specimen cut in cross section, V_H and V_V light scattering patterns were obtained as shown in Figures 4c and 4d. The V_H pattern in Figure 4c is elongated in the direction normal to the long axis of the spherulites, and the V_V pattern in Figure 4d looks like a diamond with its corners pointing both in the direction of, and perpendicular to the long axis of the cylindrical "spherulites." The V_H pattern in Figure 4c indicates that the scatterers are not spheres or disks, but are elongated objects with low length-to-diameter ratios. The scattering angle for these patterns was about 3.4°. (At this angle any characteristic scattering due to the banded structure is experimentally unobservable because the scattering falls well outside the area of the photographic film.)

More detailed interpretation of the laser light scattering patterns would require the use of laser microbeam techniques with careful selection (using micros-

(18) M. B. Rhodes and R. S. Stein, *J. Appl. Phys.*, **32**, 2344 (1961).

(19) R. S. Moore and S. Matsuoka, *J. Polym. Sci., Part C*, **5**, 163 (1964).

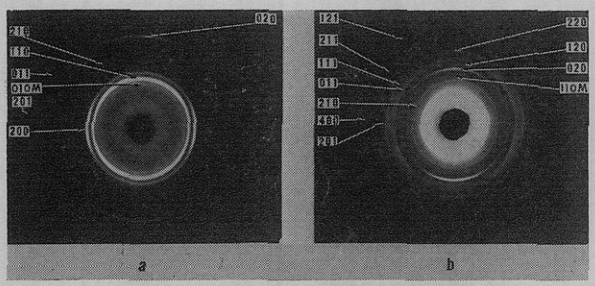

Figure 5. X-Ray diffraction diagrams of the same sample oriented as in Figure 2 with the X-ray beam normal to the page. Figure 5a was obtained at a sample-to-film distance of 5 cm and Figure 5b at 3 cm distance. Arcs of [110], [020], and [220] diffractions are found on the meridian, whereas arcs of [200], [201], and [400] (very weak) diffractions are found on the equator. The arcs of [201], [011], [111], [211], and [121] diffractions are found at an angle to the meridian and the equator. The pseudomonoclinic reflections are marked with the letter M after the *hkl* indices.

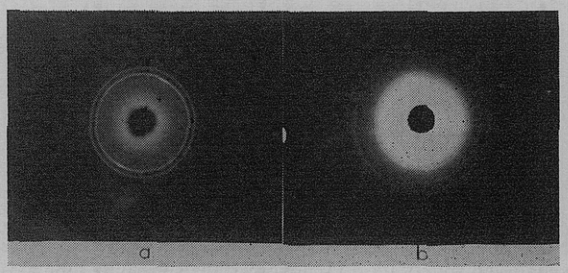

Figure 6. X-Ray diagrams of cylindrical spherulites oriented as in Figure 3. The X-ray beam was normal to the page and down the long axis of the cylindrical spherulites, *i.e.*, predominantly parallel to the lamellar long axis and the unit cell *b* axis. Figure 6a was obtained at a sample-to-film distance of 5 cm, and Figure 6b at a distance of 3 cm.

copy) of specimen regions to be irradiated by the laser beam. This difficulty arises because the population, the size, and the regularity in the arrangement of the cylindrical "spherulites" are not uniform throughout the specimens.

C. X-Ray Diffraction. With the X-ray beam normal to the *edge* of the unstretched experimental sample, *i.e.*, approximately normal to the long axis of the cylindrical "spherulites" (orientation as in Figure 2), the reflection arcs corresponding to the *hk*0 diffraction planes 110, 020, 120, and 220 occur on the meridian (the meridian is along the axis of the cylinders), as shown in Figures 5a and 5b, whereas reflection arcs corresponding to the *h*0*l* 200, 201, and 400 (very weak) diffraction planes lie on the equator. The arcs corresponding to the *hkl* 210, 011, 111, 211, and 121 diffraction planes occur at various angles with respect to the meridian. Figures 6a and 6b show X-ray diagrams of transcrystalline polyethylene taken with the X-ray beam normal to the face of the sample, *i.e.*, approximately along the long axis of the cylindrical "spherulites" with orientation as in Figure 3. Here one observes little or no preferred orientation; the reflections due to the 120 and 220 planes are missing and the reflections corresponding to the 011 and 121 planes have lower relative intensities.

The above X-ray diffraction experiments confirm that the orthorhombic unit cell *b* axis is predominantly oriented in the direction of the long axis of the cylindrical "spherulites."[10] However, judging by the absence of the *hk*0 120 and 220 diffractions and by the presence of the 200 diffraction in Figures 6a and 6b, the *b* axis direction could be at an angle as large as 30° to the spherulite long axis. A likely explanation for this is that although the average direction of the *b* axis is in the direction of the long axis of the lamellar bundles and hence along the axis of the cylindrical spherulites, lamellar twisting causes the *b* axis in one-half of the twist to occur at an angle to the lamella long axis. This is complemented by the negative of the same angle in the next half of the twist. The angular deviation probably depends on the frequency of twisting per unit length of lamella, *i.e.*, the shorter the twist distance the larger the angle between the unit cell *b* axis and the long axis of the lamella in the twisted configuration. The same holds for the other two axes of the unit cell and this, in part, could be responsible for a large azimuthal distribution of X-ray diffraction arcs. It has also been found that the twisting lamellae do not always grow exactly along the unit cell *b* axis[20-23] but can develop at an angle to it. Another possible source of the distribution of orientation arises from the manner of growth of cylindrical spherulites. The photomicrographs in Figure 2 show that the cylindrical "spherulites" start to grow as spheres in an umbrella fashion until they impinge on neighboring spherulites. From then on the growth of these "spherulites" is restricted to one direction. Thus, in the early stages of spherulite growth the fibrils gradually change their direction from perpendicular to parallel with respect to the final long axis of the cylindrical "spherulites," which also would add to the observed distribution of orientation in the X-ray diagrams. The X-ray diffraction diagrams in Figures 5a and 5b show that the meridional and equatorial diffraction arcs are long; their intensities are still significant even at 30° (azimuthal angle) to the meridian or to the equator, and they are not entirely extinct even at 90° to their intensity maxima. This indicates that, of the total number of "spherulites" exposed to the X-ray beam a significant per cent contain fibrils with a gradual distribution of angles between their long axis and the cylinder long axis.

The Pseudomonoclinic Crystalline Component. Further careful examination of X-ray diffraction diagrams reveals the presence of additional reflections which belong to a crystallographic system different from orthorhombic. The few "extra" reflections correspond to 4.56, 3.53, 2.71, and 2.08 Å units. Only the first reflection is strong enough in intensity to appear in all X-ray diagrams. The other reflections are very weak in intensity and the reflection corresponding to a *d* spacing of 3.53 Å is observed only in partially stretched samples.

In order to establish whether or not this complete set of "extra" reflections is unique to our transcrystalline polyethylene, we made a series of studies on several other polyethylenes listed in the Experimental Section. These samples had well-developed spherulitic morphol-

(20) W. D. Niegisch and P. R. Swan, *J. Appl. Phys.* **31**, 1906 (1960).
(21) P. H. Lindenmeyer, *J. Polym. Sci., Part C*, **1**, 5 (1965).
(22) H. D. Keith, *J. Appl. Phys.*, **35**, 3115 (1964).
(23) D. H. Reneker and P. H. Geil, *ibid.*, **31**, 1916 (1960).

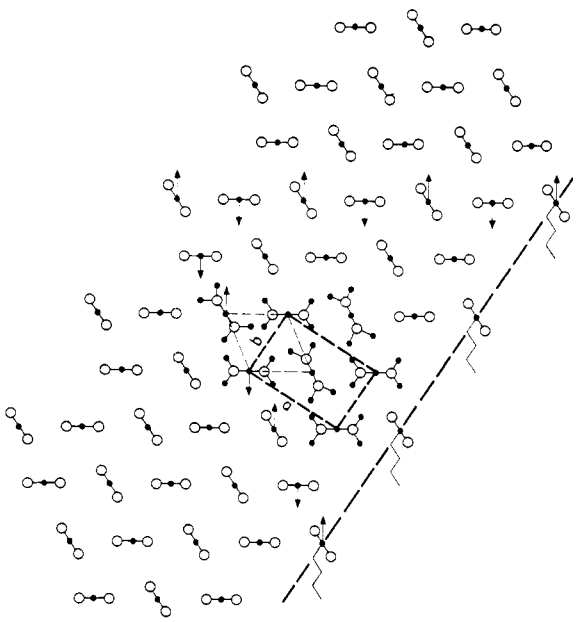

Figure 7. Schematic representation of a lattice array in a lamellar ribbon of polyethylene. The centers of the polyethylene chain ends are represented by filled-in dots between the two open circles representing the orientation of the carbon atoms. The sense of chain folding is indicated by the arrows. The *b* axis of the orthorhombic unit cell inscribed by heavy dashed lines is in the direction of the lamellar long axis. The *a* axis is in the direction of the lamella width. There are two possible directions for chain folding, along the 110 or along the $\bar{1}10$ crystallographic planes of the orthorhombic cell. The distance between the chain folds is approximately 4.51 Å in either direction as depicted by the light dashed lines. The filled-in small circles connected to only one open circle represent hydrogen atoms.

ogy, but differed in the degree of branching. X-Ray studies consistently revealed the presence of "extra" reflections in *all* samples, including a mat of polyethylene single crystals. These samples had no preferred orientation so that only the reflections at 4.56 and 2.71 Å were observed. (The reflection at about 2.08 Å nearly coincides with the *d* spacing of the orthorhombic 201 crystallographic plane; its presence can be inferred only indirectly from the higher than expected[5] intensity of this reflection.) In samples of our transcrystalline polyethylene (which has growth-induced preferred orientation), the "extra" reflection at about 2.08 Å can be distinguished from the orthorhombic 201 reflection occurring at 2.09 Å *d* spacing because of a difference in orientational positions. The "extra" reflection at about 3.53 Å *d* spacing was observed only in partially stretched samples. From these results we conclude that since the presence of this crystalline component which is not orthorhombic is common to all the forms of crystalline polyethylene we have investigated it is likely to be a feature common to all polyethylenes.

Before considering one possible manner of formation of this crystalline component and the geometry of its unit cell, we must first deal with the lattice array which gives rise to the orthorhombic unit cell. Figure 7 gives a schematic representation of such an array.

In the model of the lamellar ribbon shown in Figure 7 the successive addition of rows (or planes) of folded polymer chains results in growth such that each lamella has its longest axis coincident with the direction of the orthorhombic unit cell *b* axis. This is, of course, in accordance with the findings of a number of workers in this field.[4] The rows (or planes) of folded chains and their directions of folding lie parallel to the two diagonals in the plane of the *a* and *b* axes of the unit cell. Figure 7 suggests that the crystal growth fronts could be perpendicular to the $\bar{1}10$ or the 110 planes, or to both. It is interesting to note that the lattice rows (or planes) of chains in the two different directions in question intersect at angles closely similar to those of diamond-shaped polyethylene single crystals.

The model of Figure 7 also satisfies the polymer chain configuration in the usual orthorhombic unit cell in which the chains are parallel to the *c* axis, and the sense of the chains in the four corners is in one direction whereas the sense of the chain in the center of the cell is in the opposite direction; all this is as proposed by Bunn 30 years ago.[5]

In samples of our transcrystalline polyethylene the full twist-distance for one complete fibril rotation is found to equal approximately 30,000 Å, which corresponds to 6100 *b* axis unit cells. This gradual twist leads to the result that distortion of the α and β angles of the orthorhombic unit cell needs to be only about 0.06° to accommodate lamellar twisting. Therefore, such small deviations in the α and β angles are not large enough to require crystallization of more than a small fraction of the material in a form different from orthorhombic. The results also indicate that the observed "extra" reflections probably belong to a simpler crystallographic system than triclinic. These results led us to consider a possible skewed configuration in the *a* and *b* plane and a distortion in the γ angle of the orthorhombic unit cell as discussed below. A distortion in the γ angle could arise from the somewhat different packing of the folded polymer chains in parts of the transcrystalline material.

A lamellar ribbon diagonally skewed across its width as pictorially represented in Figure 8 could give rise to a pseudomonoclinic crystalline form. It was noted that in Figure 7 one can consider two possible directions for chain folding in the orthorhombic lattice, along the $\bar{1}10$ and 110 planes. Similarly, two possible directions for folding arise for the pseudomonoclinic system of Figure 8. If the distance between the rows of folded chains in Figure 7 were increased by about 0.21 Å and the distance between the chain folds (along orthorhombic $\bar{1}10$ plane) were decreased by about 0.28 Å then the angle between the *a* and *b* axes of the orthorhombic unit cell would need to be increased by several degrees. This, in turn, would require an expansion of the unit cell, and a modified mode of polymer chain packing in which the material existed in a pseudomonoclinic rather than an orthorhombic crystalline form. The small decrease in the distance (0.28 Å) between adjacent chains would necessitate only a very small compressive strain of each chain fold which could be readily accommodated by the fold itself. Alternatively, folding along the other possible direction would require a slight increase (0.21 Å) in the distance between adjacent chains and hence a slight dilational strain of the fold along its contour length. This could also be readily accommodated by a rearrangement of atoms along the chain contour.

Through the use of suitable computer programs we

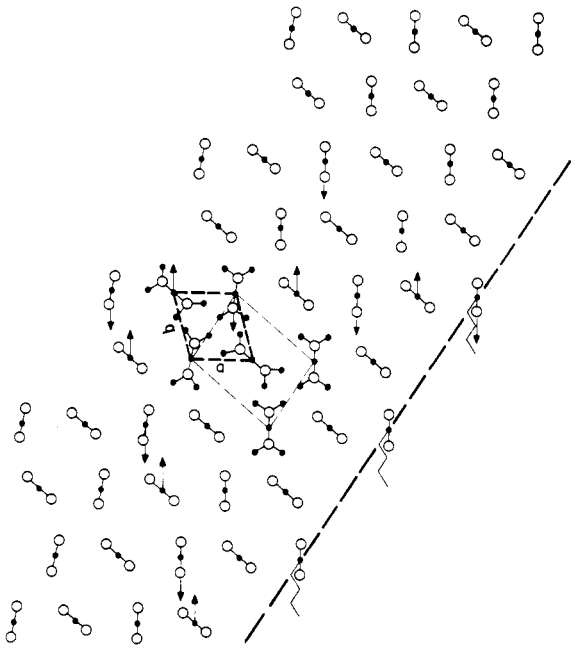

Figure 8. Schematic representation of a skewed lattice array in a lamellar ribbon of polyethylene. The symbols are the same as in Figure 7. In Figure 8 the lightly dashed lines represent a distorted orthorhombic cell in its *a* and *b* plane. The chain configuration presented here gives rise to the pseudomonoclinic unit cell depicted with heavy dashed lines. The chain folding direction is either along the *a*, or along the *b* axis of this cell.

have been successful in deriving a pseudomonoclinic unit cell for polyethylene with the following parameters: $a = 4.23$ Å, $b = 4.72$ Å, $c = 2.534$ Å, $\gamma = 105.0°$. The unit cell volume is 48.87 Å^3 and the cell contains one monomer unit. This cell accounts for *all* "extra" reflections observed in our samples of transcrystalline polyethylene (and in the other polyethylenes, as well) and also accounts for additional possible reflections whose *d* spacings are almost the same as those of the orthorhombic unit cell; therefore, some of these reflections are included in Table I under the heading of the derived pseudomonoclinic unit cell.

Judging by the intensity of the strongest "extra" reflection, which appears at 4.56 Å *d* spacing, the total amount of the pseudomonoclinic crystalline modification in our transcrystalline polyethylene is small, probably on the order of about 5–10%.

It should be pointed out that to obtain the chain packing which gives rise to our derived pseudomonoclinic unit cell, the relative orientation of the corner chains in Figure 8 must be turned by almost 90° to the original orientation of Figure 7. (It should also be noted that the derived pseudomonoclinic unit cell is diamond shaped in the *a* and *b* plane [Figure 8].) Its long diagonal is approximately parallel to the orthorhombic *a* axis and its short diagonal is in a similar disposition to the orthorhombic *b* axis. The geometry of the pseudomonoclinic unit cell and its orientational relationship to the orthorhombic unit cell *a* and *b* axes closely resemble the diamond-shaped single crystals of polyethylene and their relationship[23,24] to the orthorhombic unit cell *a* and *b* axes. Thus the 010 and 100 planes of the derived pseudomonoclinic cell are nearly coincident with the growth fronts of the diamond-shaped single crystals (sides) of polyethylene. These close similarities may turn out to be of more than coincidental significance in understanding the presence of the pseudomonoclinic component in single crystals, where lattice distortions may occur during crystallization or during drying down.

Reflections not belonging to the orthorhombic system were observed by other workers[24] (see Figure VII-35 on p 449 of ref 24) in X-ray diagrams obtained on polyethylene single crystals but were unassigned. The reflections other than orthorhombic which appear there[24] are at about 4.56 and 3.53 Å *d* spacings, as judged relative to the orthorhombic 110 and 200 reflections which are taken to correspond to spacings of 4.09 and 3.68 Å, respectively. Thus, their[24] extra reflections correspond to the 010 and $\bar{1}10$ planes of our pseudomonoclinic unit cell. In Figure VII-35 of ref 24 there are six twin reflections belonging to 110 and $\bar{1}10$ crystallographic planes of the orthorhombic system, four twin reflections of the 200 plane of the same system, and two each of the 010 and $\bar{1}10$ pseudomonoclinic reflections. The 010 reflection of the latter system will follow the

TABLE I
X-RAY DIFFRACTION RESULTS FOR THE ORTHORHOMBIC AND THE DERIVED PSEUDOMONOCLINIC UNIT CELLS OF TRANSCRYSTALLINE POLYETHYLENE

Unit cell parameters

Orthorhombic[a]	Derived pseudomonoclinic
$a = 7.36$ Å	$a = 4.23$ Å $\quad \gamma = 105.0°$
$b = 4.92$ Å	$b = 4.72$ Å
$c = 2.534$ Å	$c = 2.534$ Å
Vol. 91.76 Å^3	Vol. 48.8 Å^3
Monomer units in cell = 2	Monomer units in cell = 1

Cu Kα radiation = 1.5406 Å

d spacing, Å units				*hkl*	
Ortho	Mono	Obsd	Intensity	Ortho	Mono
	4.559[b]	4.56	M–S		010
4.090	4.086	4.09	VVS	110	100
3.680		3.68	VS	200	
	3.531[c]	3.53	VW		$\bar{1}10$
2.947		2.95	W	210	
	2.714[d]	2.71	VVW		110
2.460		2.46	S	020	
2.333		2.33	VW	120	
2.253		2.25	W–S	011	
2.196		2.19	VVW	310	
2.154	2.154	2.15	W	111	101
2.087	2.076[b]	2.08–2.09	M	201 split	$2\bar{1}0$
2.045	2.043	2.04	W	220	200
1.921		1.92	VW	211	
1.840		1.85	VVW	400	
1.763				301	
1.737				320	
1.723				410	
1.716		1.71	M	121	
1.659		1.66	W	311	

[a] The parameters of the orthorhombic unit cell were taken from E. R. Walter and F. P. Reding, *J. Polym. Sci.*, **21**, 561 (1956). [b] Appears in all samples. [c] Appears in stretched samples. [d] Appears in unstretched samples.

(24) P. H. Geil, "Polymer Single Crystals," Interscience Publishers, New York, N. Y., 1963.

orientational disposition of the orthorhombic $1\bar{1}0$ plane if both of them do occur, in fact, in the same general direction as suggested in our Figures 7 and 8. Similarly, the $1\bar{1}0$ crystallographic plane of our pseudomonoclinic cell is in the same general direction as the orthorhombic 200 plane and should follow the same orientational disposition in oriented samples if our models are correct. Figure VII-35 of ref 24 contains ample evidence that this is indeed the case; it also provides insight into the angular relationship between the two crystallographic planes of the pseudomonoclinic system and clearly supports our derived pseudomonoclinic unit cell.

The simultaneous presence of the orthorhombic component and a pseudomonoclinic component with our unit-cell dimensions would also account for certain other puzzling features observed in X-ray scattering patterns of a polyethylene single-crystal mat such as Figure VII-35 of ref 24. In particular, the reflections which occur at a spacing which nominally corresponds to the orthorhombic 110 diffraction plane should, by symmetry, be present as a set of either *four* or *eight* reflections; the presence of *six* reflections has not been explained to date. However, since the 100 plane of our pseudomonoclinic system occurs at almost exactly this same spacing one pair of the six reflections could belong to this 100 plane. Thus, the symmetry of scattering from the orthorhombic system would be preserved.

The most intense of the "extra" reflections corresponds to approximately 4.56 Å d spacing for Cu Kα radiation. This reflection and other different "extra" reflections have been reported previously, mostly in connection with results of studies of cold working carried out on polymethylenes and polyethylenes, where attempts were made to assign these reflections to a triclinic[25] and to several monoclinic[26,27] systems. Complete sets of predicted reflections were calculated for each of these crystallographic systems using the computer program. Our results indicate that these previously reported triclinic[20,25] and monoclinic[26,27] unit cells cannot correctly account for the spacings of all the "extra" reflections which we observe.

D. Spherulite Deformation. Deformation of symmetric spherulites in bulk polyethylene has been extensively investigated by a number of workers using different techniques, including light scattering.[18,19,28–31] Studies of deformation in single crystals[32,33] and spherulitic films[34] have also been carried out using other methods. However, a study of the deformation of cylindrical "spherulites" has not been carried out to our knowledge. Such a study is important not only in its own right but also in contributing to the understanding of some important aspects of morphology in deformed polyethylene by virtue of serving as a model system for certain types of deformation.

The photomicrographs shown in Figure 9 were obtained with the plane of polarization of the incident light horizontal and normal to the page, *i.e.*, across the long axis of the cylindrical spherulites.

The stretch direction was coincident with the plane of polarization of the incident light. Upon initial stretching, no significant increase was observed in the cylindrical "spherulite" diameters until about 20% sample extension had occurred (Figure 9b). Here, there was, however, a change in the relative positions of the spherulites as the stretching progressed, and the spherulites were forced to spread apart to a certain degree before their diameters increased in the direction of stress. This is plausible in terms of a morphology in which the more poorly ordered regions external to the cylinders would yield greatly under applied stress and orient in the stretching direction before the well-ordered regions showed signs of deformation. Subsequently, the diameters of the cylindrical "spherulites" increased progressively and became elliptical with the long axis of the ellipsoid oriented in the stretch direction. During this deformation the cylinders decreased in height as is shown in Figures 9a–9f, and the destruction of the cylindrical "spherulites" began at the apparently less-ordered end, the end opposite to that of nucleation. Sample necking occurred prior to 48% over-all extension. Figures 9c–9e are from the necked region. Figure 9f at 500% over-all elongation is from the end of the necked region adjacent to the fiberlike highly strained section. A decrease in the height of the cylindrical "spherulites" and their subsequent destruction is probably the result of tilting and sliding of lamellar bundles, one past the other or in bunches, in direction of stretch. More evidence for this will be provided from the analysis of X-ray diffraction results given below.

The orientation distribution of arcs in Figure 10a shows that in the unstretched sample of Figure 9a the lamellae are in a vertical position with their long axis in the same orientation as in Figure 2. The orientational dispositional of diffraction arcs in Figure 10b suggests that a significant number of lamellae become tilted at an angle to the stretch direction when the sample is strained to about 100 ± 30% over-all elongation. (The spotty strong arcs on one side of the diagram should be disregarded; they are due to diffractions from X-ray beam shielding.)

Upon further stretching, additional orientational changes occur which are shown in Figure 10c. All diffraction arcs are shorter, the arc corresponding to the 200 diffraction plane is turned by 90° relative to the unstretched state, and is found on the meridian. The 210 reflection occurs at right angles to the stretching direction instead of at 45° as in Figure 10a. The 201 reflection is found at about 45° to the stretch direction and is significantly lower in intensity. (This reflection occurs on the equator in the unstretched state (Figure 10a).) A decrease in the intensity of the 020 reflection also occurs, while the 011 reflection shows an increase in intensity. Finally, the 110 reflection occurs at 90° to the stretching direction with a very large decrease in the distribution of its orientation.

The X-ray diagram in Figure 10d was obtained with

(25) A. Turner-Jones, *J. Polym. Sci.*, **62**, S53 (1962).
(26) P. W. Teare and D. R. Holms, *ibid.*, **24**, 496 (1957).
(27) K. Tanaka, T. Soto, and T. Hara, *J. Phys. Soc. Jap.*, **17**, 873 (1962).
(28) R. S. Moore, *J. Polym. Sci., Part A*, **3**, 4093 (1965).
(29) P. Erhardt, K. Sasaguri, and R. S. Stein, *ibid., Part C*, **5**, 179 (1964).
(30) R. S. Moore and C. Gieniewski, *ibid., Part C*, **13**, 55 (1966).
(31) R. S. Moore and C. Gieniewski, *J. Appl. Phys.*, **36**, 3022 (1965).
(32) P. H. Geil, *J. Polym. Sci., Part A*, **2**, 3813, 3835 (1964).
(33) A. Peterlin, *ibid., Part C*, **9**, 61 (1965).
(34) P. Ingram, and A. Peterlin, *ibid., Part B*, **2**, 739 (1964).

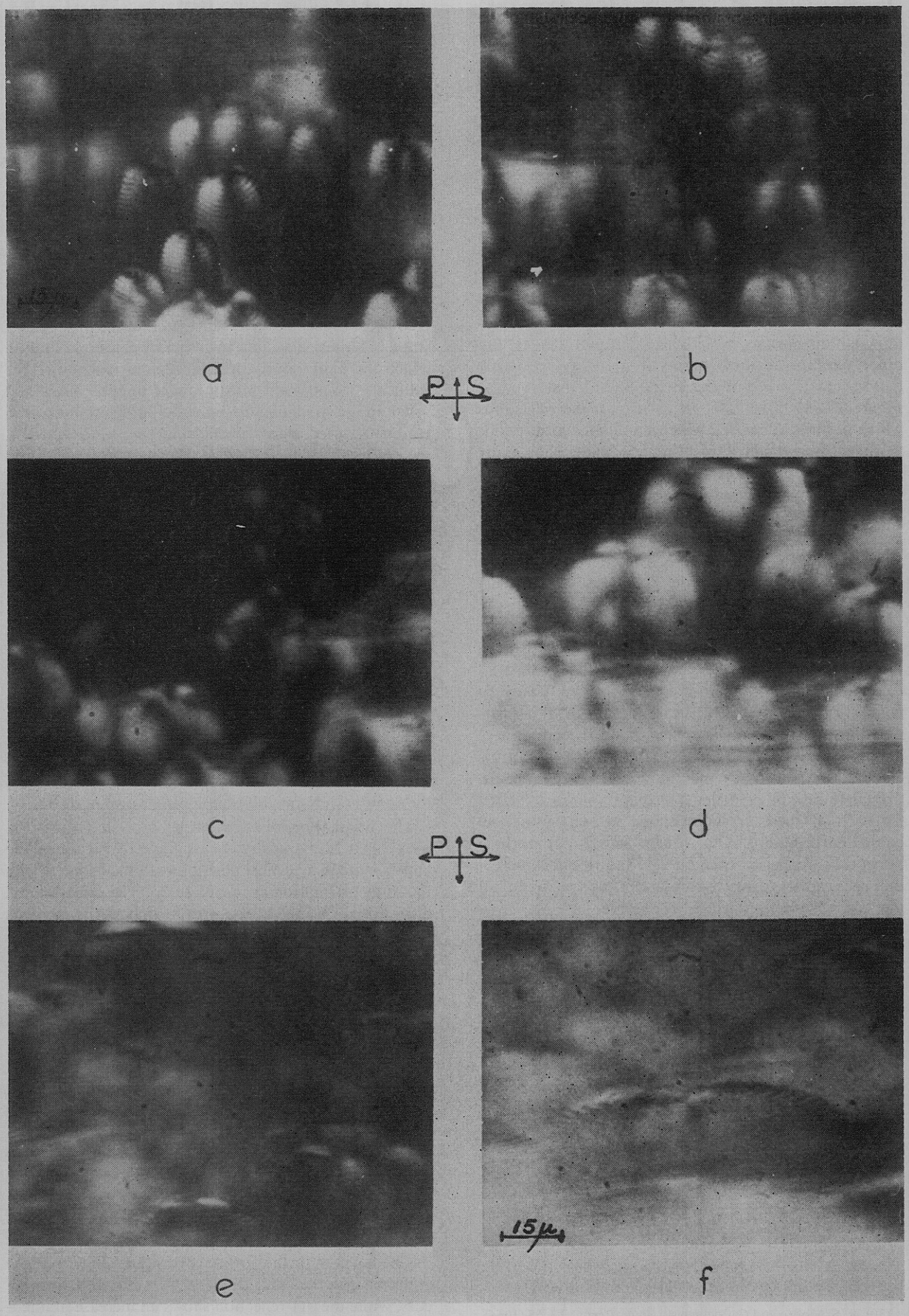

Figure 9. Crossed-polarizer photomicrographs of a cross section of a sample used in stretching. The direction of stretching and the plane of polarization were horizontal, *i.e.*, perpendicular to the long axis of the cylindrical spherulites. Over-all sample extension: (a) 0%; (b) ~21%; (c) ~48%; (d) ~76%; (e) ~100%; (f) ~500%.

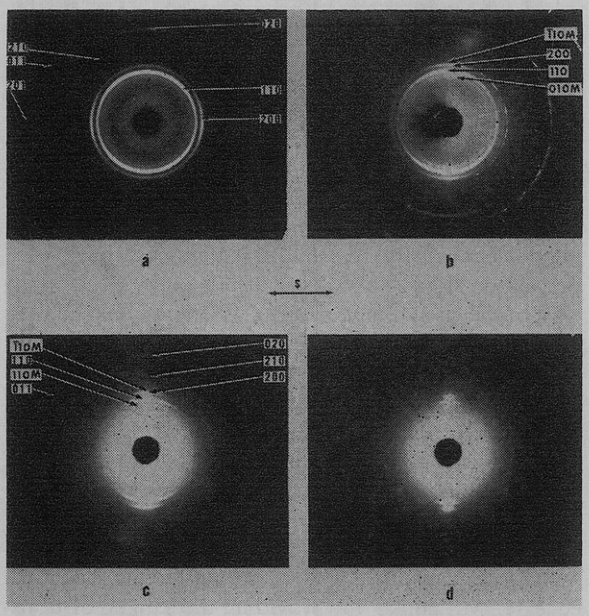

Figure 10. X-Ray diffraction diagrams of the transcrystalline sample of Figure 9 before and after stretching. The X-ray beam is normal to the plane of the paper and the spherulite long axis is vertical, as in Figures 1 and 9; the stretch direction is horizontal as in Figure 9. Figure 10: (a) unstretched; (b) X-ray beam irradiating the stretched sample just before the necked region at about 100 ± 30% over-all elongation; (c) in the necked region, over-all elongation >100%; (d) at the end of the necked region and next to the highly stretched region as in Figure 9f. The pseudomonoclinic reflections are marked with the letter M.

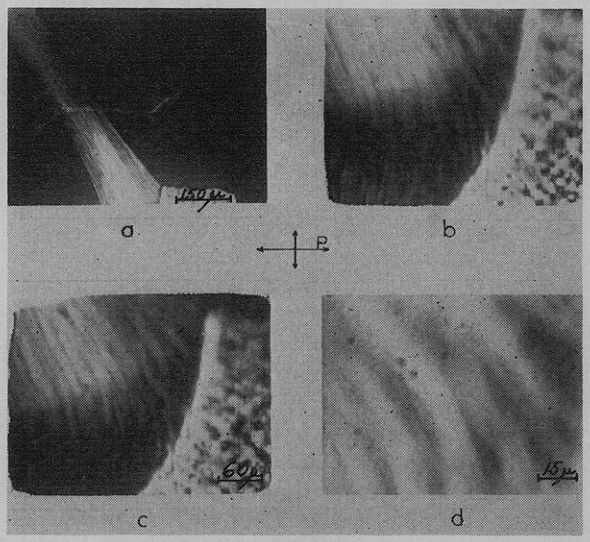

Figure 11. Crossed-polarizer photomicrographs of a specimen sectioned off the large surface of the sample, *i.e.*, across the long axis of the cylindrical spherulites. One of the corners of the specimen was stretched to an unknown degree during the microtoming operation: (b) and (c) are twice the magnification of (a). The plane of polarization of the incident light was horizontal and normal to the page. The stretched part of the specimen shows the twisted and untwisted bundles which have a fiberlike structure. The diameters of these bundles are of about the same size as the diameters of the cylindrical spherulites shown in the photomicrographs of Figures 2 and 9.

the X-ray beam irradiating the sample near the end of the necked region. The diagram is similar in many respects to a typical fiber diagram, the reflections corresponding to orthorhombic 110, 200, 210, 020, and 310 diffraction planes are at 90° to the stretching direction. The intensity of the 020 reflection has decreased to a fraction of its intensity in the unstretched sample and the 011, 111, 201, and 211 reflections are found at an azimuthal angle smaller than 45° to the stretch direction.

The orientational disposition of the reflection arcs, their relative intensities, and the changes in their intensity indicate that upon initial stretching of the sample, bundles of lamellar fibrils in transcrystalline polyethylene tilt so that their long axes tend toward the direction of stretch. Upon further stretching, as judged by microscopy, the "spherulites" become shorter due to stress induced break-up during their orientational rearrangement. Soon thereafter reorientation into a nearly fiberlike structure occurs in which the unit cell *c* axis is preferentially oriented in the draw direction, as indicated by Figure 10d. The photomicrograph in Figure 9f corresponds to the X-ray diagram in Figure 10d. Figures 9e and 9f indicate that although the spherulites are almost completely destroyed, a residue with some twisting still persists. While this mode of deformation was commonly observed in this sample, it is clear that a homogeneous deformation did not obtain over the entire specimen since no twisting was observed in the necked region.

Photomicrographs of the formation of the fiberlike structure are shown in Figures 11a–11d. These photomicrographs were obtained on a specimen sectioned off the large surface of the compression molded sample (see Figure 1), and one of the corners of this specimen was stretched to an unknown degree during sectioning. The sample area studied here is perpendicular to that shown in Figures 9a–9f. The highly stretched regions show the bundles of fiberlike structures which occur. These are twisted to different extents and are lined up approximately in the direction of stretch.

Orientation Disposition of the Pseudomonoclinic Phase. The experimental evidence for the pseudomonoclinic component of the crystalline phase was discussed in the X-ray diffraction section of this paper. This component was also found to undergo reorientation upon sample deformation. Reflections which have diffraction planes in common with those of the orthorhombic system were found to acquire similar distributions in orientation and similar changes in their relative intensities upon deformation. The disposition of these "extra" reflections during stretching adds more evidence to the existence of the pseudomonoclinic component. Thus the pseudomonoclinic 010 reflection followed the disposition of the orthorhombic 110 or $1\bar{1}0$ reflections. The pseudomonoclinic 110 reflection followed the disposition of the orthorhombic 200 reflection, and the pseudomonoclinic 110 reflection acquired a disposition similar to that of the orthorhombic 020 diffraction plane; hence these diffraction planes are in about the same general direction in their common lattice array.

The intensity of the pseudomonoclinic crystalline component is diminished in the X-ray diagram of the highly stretched sample of Figure 10d, but the component is still present. If this component arises from a

strained lattice induced by twisting of lamellar ribbons during their growth it implies that there is still a significant amount of twisting at this high degree of stretching. As suggested in Figure 9 this is probably rather localized, however.

Conclusions

The regularly banded structure around the diameter of the cylindrical asymmetric spherulites is considered to arise from a high degree of cooperative lamellar twisting, which in turn suggests a regular packing and specific orientation of the fibrillar bundles. The latter were found to run parallel to the long axis of the cylindrical spherulites.

The deformation of the cylindrical spherulites under the influence of a tensile stress normal to their long axis is explained in terms of a transformation from a spherulitic to a fiberlike structure. From X-ray diffraction and microscopy our experimental results suggest that upon sample stretching, bundles of lamellar fibrils are initially spread to a certain extent and are pulled out from the "spherulitic" aggregates. The bundles then tilt with their long axis toward the direction of stretch and untwist to an extent dependent on the degree of stretching. Soon thereafter reorientation into a new fiberlike structure occurs with the unit cell c axis preferentially oriented in the draw direction as evidenced by the X-ray diffraction results.

The small amount of a crystalline component which is different from orthorhombic and which is present in our transcrystalline polyethylene has been established to belong to a pseudomonoclinic system. The unit cell parameters for this crystalline component have been derived as shown in Table I of this paper. The presence of the pseudomonoclinic crystalline component is common to all the forms of crystalline polyethylene we have investigated and is likely to be a feature common to all polyethylenes. A possible mode of formation of this component has been suggested in terms of a somewhat different packing of the folded polymer chains in a strained lattice array.

Acknowledgments. The authors gratefully acknowledge H. M. Zupko for providing the sample of transcrystalline polyethylene and L. S. Frishkopf and Mrs. H. S. Hanes for providing sectioned specimens of this sample.

The Effect of Salts and of Adenosine 5′-Triphosphate on the Shortening of Glycerinated Muscle Fibers[1]

L. Mandelkern and E. A. Villarico

Department of Chemistry and Institute of Molecular Biophysics, Florida State University, Tallahassee, Florida. *Received March 21, 1969*

ABSTRACT: Studies of the length–temperature–composition relations for a glycerinated muscle fiber (rabbit psoas) in various salt solutions and in ATP are reported. Despite the morphological complexities inherent to this fibrous system, complete shortening is shown to be a consequence of a cooperative structural transition similar to that observed with the other fibrous proteins. The results obtained with the salt solutions help establish the transition temperature in the absence of added monomeric species, *i.e.*, in pure water. Under these conditions, the transition occurs at an elevated temperature. It is, however, found that this transition temperature is lowered monotonically with the addition of increasing amounts of ATP. Complex transition temperature–composition relations are observed when the supernatant solution contains either Mg^{2+} or Ca^{2+} in conjunction with ATP.

It has been established[2] that the fibrous proteins such as collagen, elastoidin, and the α and β keratins undergo a cooperative structural transition at a characteristic temperature which depends on the nature and composition of the medium in which they are immersed. This transformation involves the disruption of a highly axially oriented ordered structure into one which is disordered. All the general manifestations of a first-order phase transition are displayed and a large diminution in length usually accompanies the process. This latter observation is a consequence of the major conformational differences of the constituent macromolecules in the two states. A variety of reagents, known to be effective in disrupting the ordered structure of dilute protein and polypeptide solutions, also induces the transformation in the macroscopic fibrous systems.[2b]

The muscle fiber system, which has a characteristic α-keratin-like wide-angle X-ray diffraction pattern, is morphologically and chemically more complex than the other protein fibers studied. It contains at least two major protein constituents, and the unique morphology of striated muscle has been described in detail.[3] Specific to this fibrous system, shortening can be induced by the addition of ATP[4] and the catalytic hydrolysis of this species is effected during the process. Although major structural and compositional differences between muscle and the other fibrous proteins are recognized, it has been

(1) This research was supported in part by a grant from the U. S. Public Health Service, GM 10614, and a contract with the Division of Biology and Medicine, Atomic Energy Commission.

(2) (a) L. Mandelkern, *Ann. Rev. Phys. Chem.*, **15**, 421 (1964); (b) L. Mandelkern, *J. Gen. Physiol.*, **50**, No. 6 (Part 2), 29 (1967).

(3) H. E. Huxley and J. Hanson in "Structure and Function of Muscle," Vol. 1, G. H. Bourne, Ed., Academic Press, New York, N. Y., 1960, p 183.

(4) Abbreviation used in this work: ATP, adenosine 5′-triphosphate.